Chemical Science

EDGE ARTICLE

View Article Online
View Journal | View Issue

Cite this: *Chem. Sci.*, 2018, **9**, 5479

The 3rd degree of biomimetism: associating the cavity effect, Zn^{II} coordination and internal base assistance for guest binding and activation†

A. Parrot,[a] S. Collin,[a] G. Bruylants[b] and O. Reinaud*[a]

The synthesis and characterization of a resorcinarene-based tetra(imidazole) ligand is reported. The properties of the corresponding Zn^{II} complex are studied in depth, notably by NMR spectroscopy. In MeCN, acid–base titration reveals that one out of the four imidazole arms is hemi-labile and can be selectively protonated, thereby opening a coordination site in the *exo* position. Quite remarkably, the 4th imidazole arm promotes binding of an acidic molecule (a carboxylic acid, a β-diketone or acetamide), by acting as an internal base, which allows guest binding as an anion to the metal center in the *endo* position. Most importantly, the presence of this labile imidazole arm makes the Zn^{II} complex active for the catalyzed hydration of acetonitrile. It is proposed that it acts as a general base for activating a water molecule in the vicinity of the metal center during its nucleophilic attack to the *endo*-bound MeCN substrate. This system presents a unique degree of biomimetism when considering zinc enzymes: a pocket for guest binding, a similar first coordination sphere, a coordination site available for water activation in the *cis* position relative to the substrate and finally an internal imidazole residue that plays the role of a general base.

Received 9th March 2018
Accepted 29th May 2018

DOI: 10.1039/c8sc01129j

rsc.li/chemical-science

Introduction

Nature has selected proteic structures with remarkable properties for molecular recognition and catalysis. Their structural identification gives key insights into active sites, which is helpful for understanding structure/reactivity relationships. It is also an inexhaustible source of inspiration for chemists interested in the design of smart systems prone to recognition or catalysis, or both. The classical approach to mimic metallo-enzymes consists in the elaboration of a ligand that reproduces the first coordination sphere of the natural system.[1–5] Control of the second coordination sphere has recently become a hot topic and has been recognized as a key point for substrate/ligand stabilization or activation.[2,3,5–13] We have developed a biomimetic supramolecular approach consisting in the association of a macrocyclic cavity to a biomimetic coordination core in order to control the second coordination sphere (and further) with a macrocyclic structure surrounding the metal ion labile site. This approach also allows controlling the access to the metal ion and thus the selectivity against ligands. The first system we developed uses a calix[6]arene as a funnel to drive the exogenous ligand to the metal ion. In this system, a single guest can bind to the metal ion (Fig. 1).[14,15] More recently, we have described systems based on resorcinarenes.[16,17] The so-called bowl complexes, presenting three imidazole arms on their large rim,[18] were shown, when complexing a zinc cation, to present two labile sites in the *cis* position relative to each other, which opened new opportunities for recognition and reactivity.[19–23]

In many metallo-enzymes however, the catalytic cycle involves a general base (or acid) carefully positioned vis-à-vis the substrate. Zinc hydrolytic enzymes, in particular, generally display a N_2O or N_3 coordination core, associated with a general base which is hydrogen-bonded to a water ligand (Fig. 2).[24] The latter is often a Glu or Asp residue but in some cases, it is a His residue as for families of histone deacetylases[25,26] and metallo-β-lactamases.[27] In some enzymes, this general base (an Asp residue) is coordinated to the metal ion, as in adenosine deaminase.[28] It has been shown to assist the water nucleophilic attack to the coordinated substrate (*e.g.* the carbonyl group of a peptidic bond, acetamide moieties or even the pyrimidine group of a nucleic base) as schematized in Fig. 2. Hence, the key features for the enzymatic activity stem from the strong Lewis acidic center, the presence of two labile sites in *cis*-position relative to each other and from the general base present in the first or second coordination sphere. This pattern allows the simultaneous activation of the electrophilic substrate and the

[a]*Laboratoire de Chimie et Biochimie Pharmacologiques et Toxicologiques, CNRS UMR8601, Université Paris Descartes, Sorbonne Paris Cité, 45 rue des Saints Pères, 75006 Paris, France. E-mail: olivia.reinaud@parisdescartes.fr*

[b]*Engineering of Molecular NanoSystems, Ecole Polytechnique de Bruxelles, Université Libre de Bruxelles (ULB), Avenue F. D. Roosevelt 50, CP165/64, B-1050 Brussels, Belgium*

† Electronic supplementary information (ESI) available: Full NMR spectra, DOSY, IR, and ITC titrations. See DOI: 10.1039/c8sc01129j

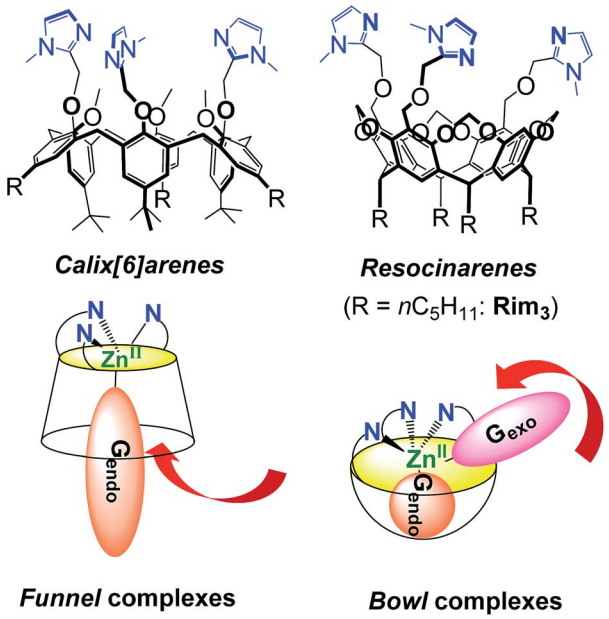

Fig. 1 Compared structures and hosting properties of cavity complexes based on calix[6]arene (left) and resorcinarene (right) functionalized with three imidazole moieties that mimic proteic active sites. The red arrows emphasize the different guest binding pathways. G stands for a guest ligand.

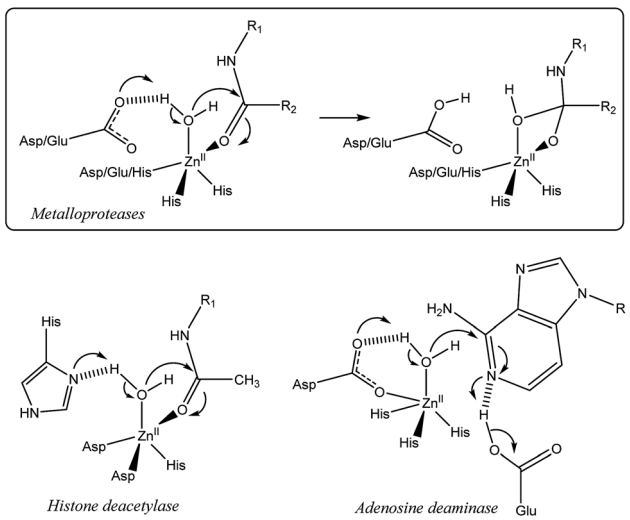

Fig. 2 Top: generic active site of Zn^{II} proteases and the key step involving the assistance of an Asp or Glu residue as a general base. Bottom: example of variations of the active site and nucleophilic attack occurring in other zinc hydrolytic enzymes.

water nucleophile. Upon coordination, both the carbonyl substrate and the water ligand are polarized, whereas the general base activates the water nucleophile to provide the tetrahedral oxyanion intermediate, which is stabilized by coordination to Zn^{II}.

Here, we present the new bowl ligand **Rim$_4$** (Scheme 1) that displays a fourth imidazole arm. Studies with the corresponding Zn^{II} complex show that, whereas three imidazole groups

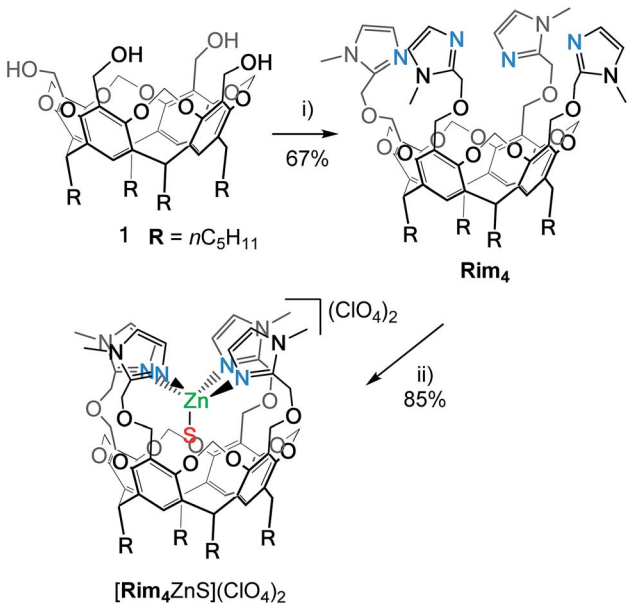

Scheme 1 Synthetic route for ligand **Rim$_4$** and its corresponding Zn^{II} complex. (i) NaH, 2-chloromethyl-1-methyl-1*H*-imidazole, and DMF. (ii) $Zn(OH_2)_6(ClO_4)_2$ and EtOH. S stands for solvent (EtOH here) or residual water.

allow the strong binding of the metal center at the entrance of the cavity, the 4th imidazole arm is hemilabile and can act as an internal base. The consequences on molecular recognition and hydrolytic activity towards the acetonitrile guest are presented and discussed in the context and development of biomimetic catalysts.

Results and discussion

Synthesis of Rim$_4$ and complexation of Zn^{II}

The resorcin[4]arene tetra(imidazole) ligand **Rim$_4$** was synthesized by reacting the tetra(alcohol) precursor **1** [29] with 2-chloromethyl-1-methyl-1*H*-imidazole in the presence of NaH (Scheme 1).

The zinc complex was obtained by reacting **Rim$_4$** with one equivalent of Zn^{II} perchlorate salt in EtOH. The complex, [**Rim$_4$**Zn(EtOH)]$(ClO_4)_2$, spontaneously precipitated out of the solution as an off-white solid. The complex was fully characterized by NMR, IR, and ESI-MS. IR analysis confirmed the presence of ClO_4^- counterions. **Rim$_4$**Zn was only soluble in CD_3CN, displaying a well-defined signature, corresponding to a complex with an apparent C_{4v} symmetry (Fig. 3), even at 240 K. Only two aromatic signals are assigned to the imidazole, showing that all four imidazoles are equivalent on the NMR chemical shift timescale. NMR experiments in CH_3CN with 5% CD_3CN showed the coordination of acetonitrile to zinc, with an intracavity peak at −2.20 ppm (see ESI Fig. S32†). The corresponding complexation induced shift (CIS = −4.14 ppm), due to the embedment of the guest methyl group in the bowl cavity, is similar to that measured with **Rim$_3$** (δ = −2.14 ppm, CIS = −4.08 ppm). The presence of exactly one equivalent of free ethanol is likely due to its initial hosting in the cavity (in the

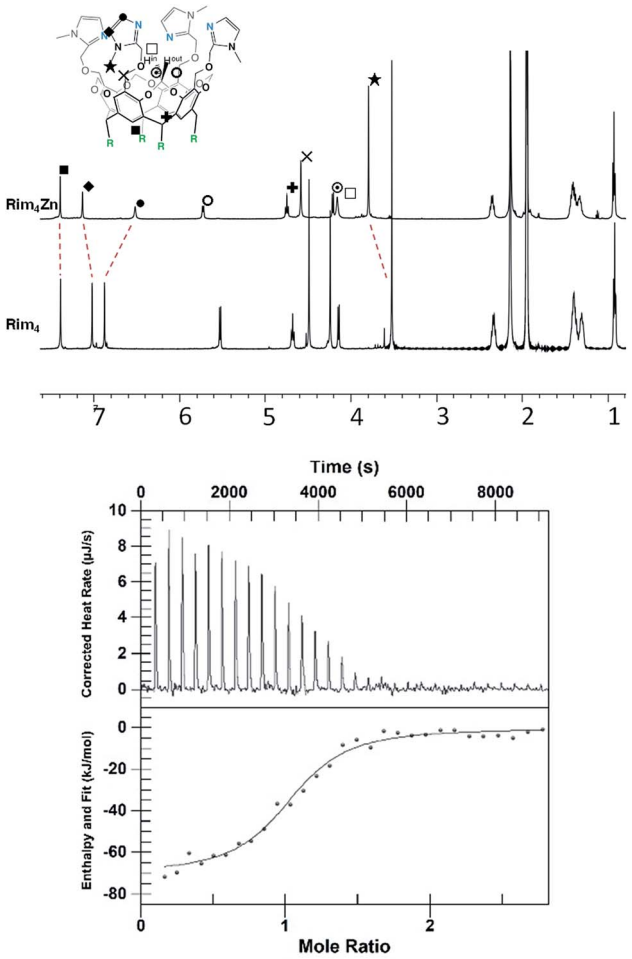

Fig. 3 Top: ^{1}H NMR spectra (600 MHz, 300 K, CD_3CN) of ligand **Rim$_4$** and its corresponding Zn^{II} complex, [**Rim$_4$**Zn(MeCN)]$(ClO_4)_2$. Bottom: titration of **Rim$_4$** (0.05 mM) with zinc perchlorate (0.5 mM) in dry MeCN.

as-isolated complex) and substitution by the coordinating solvent. DOSY experiments conducted on **Rim$_4$** and its Zn^{II} complex in MeCN showed similar diffusion coefficients (7.6×10^{-10} and 7.4×10^{-10} m^2 s^{-1}, respectively).‡ Zn^{II} complexation to the bowl ligands **Rim$_3$** and **Rim$_4$** was also monitored by isothermal calorimetry (ITC, Fig. 3) in dry acetonitrile. In each case, the Zn^{II} complexation, confirmed to be of 1 : 1 stoichiometry, appeared to be enthalpically driven ($\Delta H^\circ \approx -70$ kJ mol^{-1}) with a large entropic penalty (Table 1).

The similarity of the thermodynamic profiles suggests that the fourth imidazole does not play a crucial role in the complexation and is only weakly bound to the metal center.§

Table 1 ITC data for **Rim$_3$** and **Rim$_4$** titrated with zinc perchlorate in dry acetonitrile at 25 °C

Compound	ΔH° (kJ mol^{-1})	K (M^{-1})	n	ΔS° (J mol^{-1} K^{-1})
Rim$_3$	-67 ± 5	$(6 \pm 4)\ 10^6$	0.9 ± 0.2	-102 ± 26
Rim$_4$	-69 ± 7	$(7 \pm 2)\ 10^5$	1.0 ± 0.1	-120 ± 23

Acid–base studies

Acid titration of [**Rim$_4$**Zn(MeCN)]$(ClO_4)_2$ was first conducted with a strong, non-coordinating acid, namely picric acid, and monitored by ^{1}H NMR and ITC (Fig. 4). The addition of the first equivalent of acid led to a shift of the imidazole resonances, which is particularly pronounced for the proton in the α-position of the coordinating nitrogen atom (signal at 6.5 ppm). The fact that the other peaks are little affected suggests that the coordination of Zn^{II} to **Rim$_4$** is maintained, whereas the imidazole set sees its global environment changed. One explanation is that one imidazole undergoes protonation, whereas the three other imidazoles maintain the Zn^{II} bound to the bowl structure. The fact that only one set of resonances for the imidazole arms is observed is best explained by a fast exchange (*vs.* the NMR chemical shift time scale) between the protonated and the coordinated ones. Such a "dancing" behavior was observed with the **Rim$_3$**Cu^{I} complex where the Cu^{I} ion is 2-coordinate in a non-coordinating solvent.[30] Above 4 equivalents of acid, a new sharp signature is obtained, which corresponds to the fully protonated ligand, as attested to by a low-field resonance at *ca.* 13 ppm accounting for 4 protonated imidazolium arms. Interestingly, between 2 and 4 equivalents of acid, the emergence of new peaks (indicated by arrows) shows the co-existence of the Zn^{II} complex and the tetraprotonated ligand that are in slow exchange relative to the chemical shift time scale. The ITC study, conducted at a much lower concentration (Fig. 4, right), evidenced a clean exothermic event (−26 kJ mol^{-1}) for the mono-protonation, which also appears entropically favorable ($\Delta S^\circ = 23$ J K^{-1} mol^{-1}). Considering a pK_a value of 11 for picric acid in MeCN, the pK_a corresponding to the imidazolium arm can be estimated to be 16.7.¶[31] Although the pK_a of imidazole in MeCN has not been reported (6.95 in water), it can be compared to those of 2-NH_2-benzimidazole (15.95 in MeCN *vs.* 7.51 in water) and 2-NH_2-pyridine (*ca.* 14.5 in MeCN *vs.* 6.75 in water).[32] The similarity of the values in MeCN further confirms the weak coordination of this fourth imidazole arm to the metal ion. Note that the protonation reaction is fully reversible since subsequent addition of a base such as NEt_3 led to the quantitative regeneration of the Zn^{II} complex.

Reaction of the Zn^{II} complex with acetic acid was then studied. Indeed, acetic acid is a weak acid, but a potentially coordinating guest. With **Rim$_3$**, it was shown that the Zn^{II} center displays very strong affinity for this guest provided a base (triethylamine) was added to the solution, leading to the formation of the monocationic [**Rim$_3$**Zn(OAc)]$^+$ adduct.[33] Having evidenced the lability of the fourth imidazole arm of complex [**Rim$_4$**Zn(MeCN)]$^{2+}$ mediated by the addition of a strong acid, we explored the possible concomitant deprotonation/coordination of AcOH by the complex based on **Rim$_4$**.

Upon stepwise addition of acetic acid to a solution of [**Rim$_4$**Zn(MeCN)]$^{2+}$ in acetonitrile, two new resonances appeared in the high-field region [δ(Me) = −2.25 and −2.38 ppm] of the ^{1}H NMR spectra (Fig. 5, bottom), attesting to the inclusion of acetate into the resorcinarene cavity. Concomitantly, new peaks emerged in the aromatic region, which evidenced the formation of three different species. According to

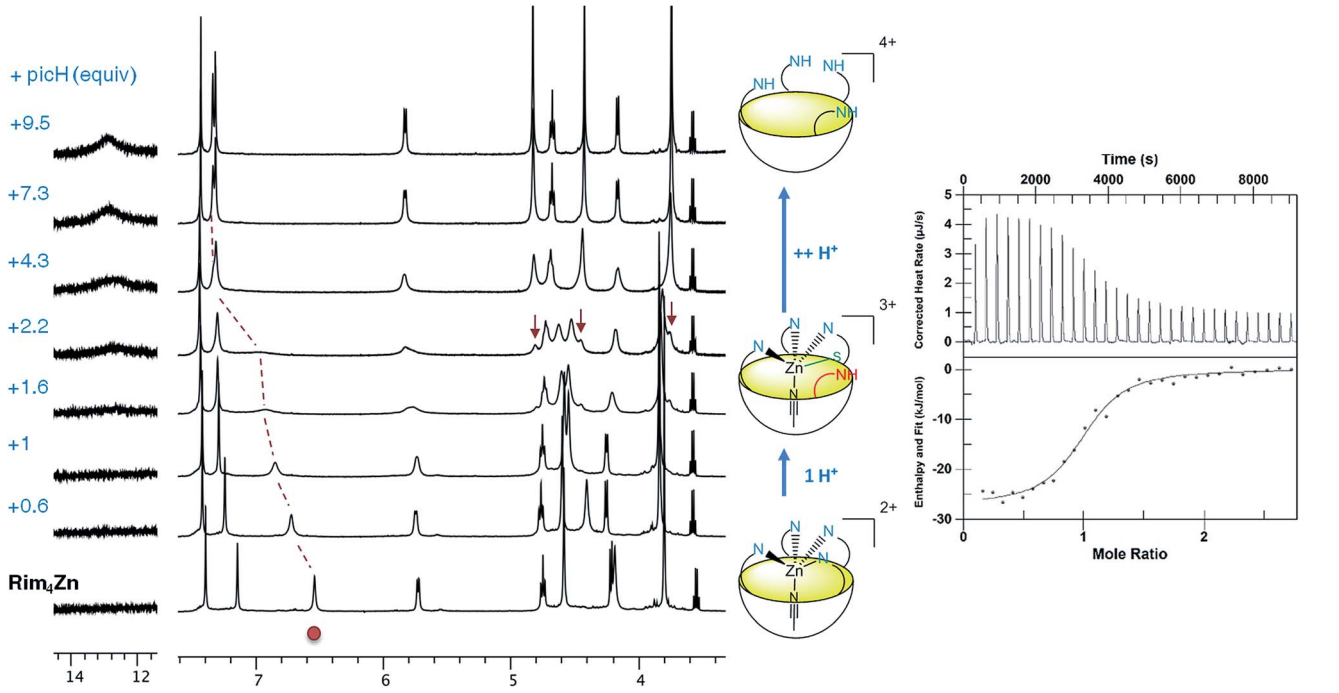

Fig. 4 Titration of $[\mathbf{Rim_4}Zn(MeCN)](ClO_4)_2$ with picric acid in CD_3CN at 300 K. Left: ^1H NMR monitoring (2 mM, 500 MHz). The red dot depicts an imidazole peak; the little red arrows indicate growing peaks assigned to the fully protonated ligand. Right: ITC monitoring of the monoprotonation of the complex (0.05 mM) by picric acid (PicH, 0.5 mM): $K = 5.44 \times 10^5\ M^{-1}$ ($n = 0.93$), $\Delta H^\circ = -26$ kJ mol^{-1}, $\Delta S^\circ = 23$ J K^{-1} mol^{-1}; $pK_a = -5.7$ (which gives $pK_a = 16.7$, considering pK_a(PicH) = 11.0 in MeCN).

integrations of the imidazole peaks relative to *endo*-bound acetate, one set of imidazole resonances corresponds to the major peak (−2.25) at one equivalent of added acetic acid (identified with large red dots in Fig. 5), whereas the other sets correspond to the minor peak ($\delta = -2.38$ ppm). Lastly, the appearance of a low field resonance at 12.4 ppm (see ESI Fig. S21†) indicated the protonation of one imidazole moiety. All of this information accounts for the quantitative coordination of acetate in the cavity accompanied by the protonation of one imidazole arm. The three associated dicationic acetato complexes actually correspond to different solvated forms. Indeed, we have previously shown that the analogous tris(imidazole) Zn^{II} complex, based on the **Rim$_3$** ligand,[33] can bind exogenous donors in the *exo* position, such as solvent (MeCN) or residual water. Here, the protonation of one imidazole arm opens a coordination site in the *exo* position that can be free (major species under these experimental conditions {$[\mathbf{Rim_4}HZn(OAc)]^{2+}$}, or occupied by solvent or residual water {$[\mathbf{Rim_4}HZnS(OAc)]^{2+}$}). This was further confirmed by water addition to a solution containing the acetato dicationic complex, which induced growth of the high-field peak at $\delta = -2.38$ ppm, and was thus attributed to the water adduct (S = H_2O, see ESI Fig. S22 and S23†).

In order to confirm all these observations, subsequent titration of the protonated acetato complex with a base was conducted (Fig. 5, top). Upon progressive addition of Et_3N, all resonances converged towards a major set corresponding to the monocationic acetato complex $[\mathbf{Rim_4}Zn(OAc)]^+$. Indeed, a similar signature was obtained upon addition of AcONa to the nitrilo complex (see ESI Fig. S9†). The resonance at 12.4 ppm corresponding to the protonated imidazolium arm vanished, whereas those corresponding to Et_3N (at 3.1 ppm) attested to its quantitative protonation (see ESI Fig. S21†). The solvated species almost disappeared, in agreement with the deprotonation of the fourth imidazole arm that favors its coordination to the detriment of exogenous donors.

Probing metal access and basic assistance

Size selectivity. Like in the case of **Rim$_3$**-based metal complexes, the presence of the resorcinarene bowl structure confers size-selectivity for guest binding.[33] Indeed, only formic and acetic acid readily led to the corresponding *endo*-complexes, not larger carboxylic acids such as propanoic acid. Noteworthy however, the **Rim$_4$**Zn^{II} complex coordinates the propionate anion under the same conditions, denoting a slightly different positioning of the metal ion relative to the bowl cavity.

Basic assistance. The basic assistance for guest binding was evaluated with a donor presenting a higher pK_a, namely acetamide.‖ With **Rim$_3$**, the latter was shown to bind to the Zn^{II} center only in the presence of Et_3N.[33] With **Rim$_4$**, addition of acetamide readily led to the formation of the *endo* complex as shown by the appearance of a high-field peak at −2.40 ppm that attests to the inclusion of the methyl group of acetamide (CIS = −4.25 ppm; Fig. 6c).

As in the case of the **Rim$_3$**-based acetamido complex, several sets of peaks corresponding to the associated **Rim$_4$** core in the

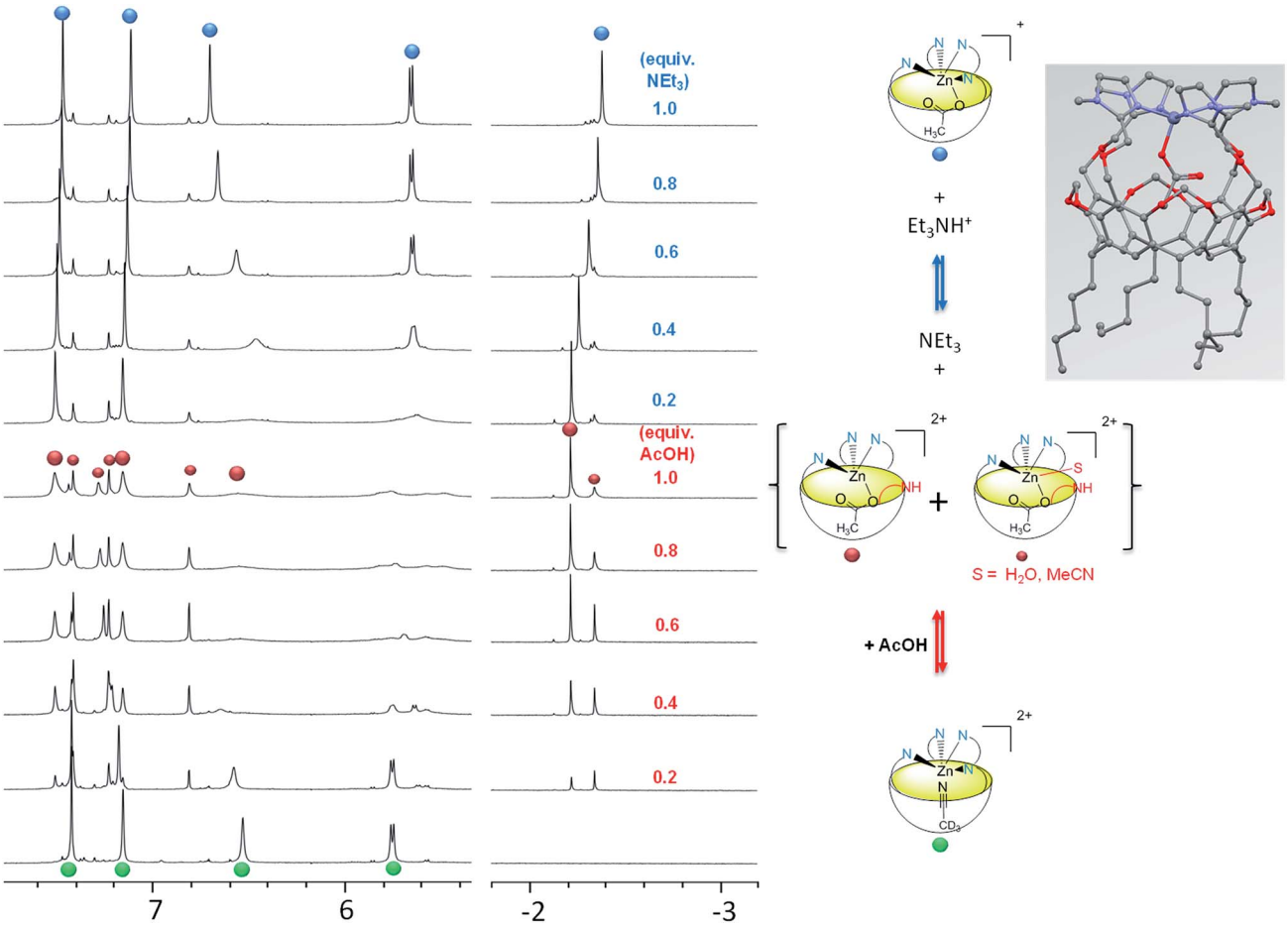

Fig. 5 Coordination of acetate by $[\mathbf{Rim_4}Zn(MeCN)](ClO_4)_2$ in CD_3CN and evidence of the hemilability of the 4th imidazole arm. Left: ^1H NMR titration (500 MHz, 300 K, CD_3CN) of $[\mathbf{Rim_4}Zn(MeCN)](ClO_4)_2$ with (from bottom to top) acetic acid, and subsequent titration with Et_3N. The small red dots are attributed to the solvated dicationic acetato species (S = H_2O or MeCN). Right: various species observed during the titrations. Inset: model of the acetato complex $[\mathbf{Rim_4}Zn(OAc)]^+$ obtained with software HyperChem.[34]

δ = 4–8 ppm region denote the presence of different species attributed to different coordination modes of the acetamido guest. Addition of Et_3N affected the $\mathbf{Rim_4}$ signature but not the guest resonance (Fig. 6d), thus confirming its coordination as an anion.**

Bidentate coordination. In order to probe the relative position of the *endo* and *exo* sites open for exogenous donor binding (*e.g.* guest in the *endo* position and solvent in the *exo* position), coordination of bidentate guests was scrutinized.

Acetyl- and benzoylacetone, which were shown to readily bind to the $\mathbf{Rim_3}Zn^{II}$ complex in a bidentate fashion in the presence of Et_3N,[33] were tested with the $\mathbf{Rim_4}Zn^{II}$ complex. As for carboxylic acids and acetamide, direct titrations showed upfield methyl peaks attesting to the coordination of both β-diketones, and concomitant broadening and down-field shifts of the imidazole resonances. Upon subsequent addition of Et_3N, all peaks sharpened, and the corresponding NMR signatures attested to the formation of the monocationic host–guest adducts (Scheme 2). For acetylacetone, a variable temperature study evidenced concomitant broadening (as T increases) of the peaks at $\delta = -2.56$ ppm and 1.78 ppm, attributed to the methyl groups of the guest in *endo* and *exo* positions, respectively. This indicates that these methyl groups are in dynamic exchange. As previously described with $\mathbf{Rim_3}$, the acetylacetonate guest undergoes an intramolecular exchange, with its *endo* and *exo* methyl groups switching positions.[34] For benzoylacetone, due to the cavity size, the phenyl group sits in the *exo*-position, as indicated by the corresponding low CIS values (−0.09 ppm for phenyl and −0.33 for CH), while the methyl group is selectively bound in the *endo*-position (CIS = −4.05 ppm). Finally, the apparent C_{4v} signature attests to the fast exchange of the imidazole groups in the vicinity of the metal ion, even at low T (240 K).††

In summary, in MeCN and in the absence of a specific guest, the $\mathbf{Rim_4}Zn^{II}$ complex presents the following characteristics:

– Three imidazole arms maintain firmly the metal center above the cavity, at its entrance.

– A molecule of solvent (MeCN) is bound in the *endo* position and is exchangeable.

– The fourth imidazole is labile and reacts readily as a base. It can promote the coordination of poorly acidic guests and their binding as an anion. It is interesting to consider the corresponding host–guest process from the acid–base point of view: the ^1H NMR studies showed quantitative guest binding

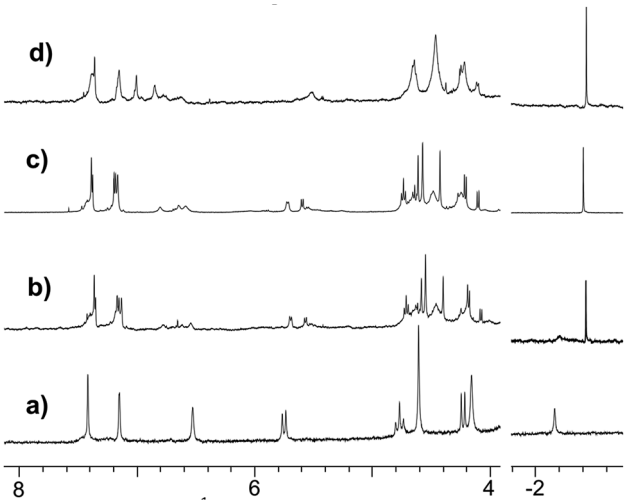

Fig. 6 Comparative ^{1}H NMR signatures (250 MHz, 300 K) of the nitrilo and acetamido **Rim$_4$Zn^{II}** complexes in acetonitrile: (a) the initial spectrum of the freshly dissolved nitrilo complex in CH_3CN + 5% CD_3CN; (b) spectrum of the **Rim$_4$Zn^{II}** complex (4.7 mM) in CH_3CN + 5% CD_3CN after two weeks at RT; (c) a fresh solution of the **Rim$_4$Zn** complex dissolved in CD_3CN to which 1.5 equiv. of CH_3CONH_2 was added; and (d) the same sample to which 1 equiv. of Et_3N was added.

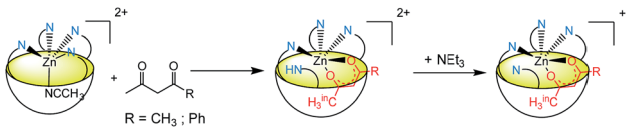

Scheme 2 Coordination of diketones to [**Rim$_4$Zn**(MeCN)](ClO$_4$)$_2$ in MeCN.

upon addition of *ca.* 2 equiv. of acidic guest GH at 2 mM in MeCN (Fig. 7). This indicates that the corresponding equilibrium constant is greater than 10^4 M^{-1}. For comparison, the proton exchange between acetamide (GH) and simple imidazole in a non-protic solvent (DMSO) is *ca.* 10^{-19}. Hence, the association of Lewis acid coordination, cavity-hosting and internal base of the **Rim$_4$Zn^{II}** system allows displacing the acid–base equilibrium by a factor higher than 10 (ref. 23)!

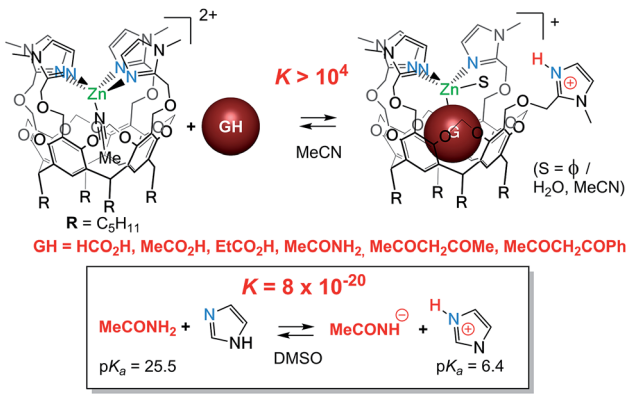

Fig. 7 Basic assistance for acidic guest binding and comparison with a simple acid/base equilibrium.‖

– Lastly, the two coordination sites open for guest binding are in the *cis* position relative to each other. One site is in the *endo*-position under the steric control of the bowl cavity, and the other one is in the *exo* position, exposed to the solvent.

All these characteristics are highly reminiscent of the active site of hydrolytic enzymes, which drove us to explore its reactivity.

Acetonitrile hydration

The reactivity of the nitrilo [**Rim$_4$Zn**(MeCN)]$^{2+}$ complex towards water was first scrutinized by ^{1}H NMR spectroscopy. After two weeks at room temperature, the NMR signature of the nitrilo complex [in CH_3CN containing 5% CD_3CN and residual water (around 0.1%)] was replaced by that of the acetamido complex (Fig. 6a and b). GC-MS analyses of the solution (following a literature procedure)[35] confirmed the formation of acetamide.

The hydration reaction was then studied at 70 °C by ^{1}H NMR spectroscopy with various contents of water. With **Rim$_4$Zn^{II}** (3.8 mM), in CH_3CN/H_2O (8 : 2 v/v) and after 6 days at 70 °C, new broad signals at 6.15 and 5.59 ppm were observed and a sharp peak at 1.84 ppm appeared. This indicated the presence of free acetamide, the singlet at 1.84 ppm corresponding to the methyl group and the broad signals to the NH_2 moiety, which was confirmed by IR, HMBC, HSQC and ^{13}C experiments (see ESI Fig. S32–37†). Integration of the peaks indicated the formation of 7 equivalents of acetamide after 14 days at 70 °C. Under the same conditions, no reaction was observed using 3 mM Zn(ClO$_4$)$_2$ or 3 mM **Rim$_3$Zn^{II}** instead of **Rim$_4$Zn^{II}**, even in the presence of an additional base (*N*-methyl imidazole). Kinetic studies were conducted by ^{1}H NMR spectroscopy with DMF as an internal reference for acetamide quantification. The recorded data revealed a 2-phase kinetics (Fig. 8): a burst phase from 0 to 10 minutes corresponding to the formation of the first equivalent of acetamide ($t_{1/2}$ = 4 min), which is *endo*-bound. After 10 minutes, the reaction slowed down significantly. This suggests that the *endo*-bound acetamide partially inhibits the reaction due to cavity filling. Increasing the catalyst concentration by a factor of two doubled the reaction rate in agreement with first-order kinetics with respect to the complex. This two-phase kinetics is well described by a classical model for reaction inhibition due to product displacement (see the ESI†),[36] and the associated reaction rates for each phase are reported in Table 2. Whereas the water content seems to have little impact on the burst phase, it enhanced the reaction rate in the second phase, reaching a TOF of 0.22 h^{-1} at 35% H_2O (highest water percentage for solubility reasons).

When conducted in D_2O, no change in the reaction rates was detected, which means no (or very little) isotopic effect for the hydration reaction.

Based on all of this information, a mechanism is proposed in Scheme 3.

The addition of water leads to a decrease of MeCN occupancy: with 5% water content, only 50% of the resorcinarene sites are occupied by MeCN, and with 20% water content, the major species is the aqua complex A. This complex is in fast equilibrium with the nitrilo complex B (as evidenced by NMR

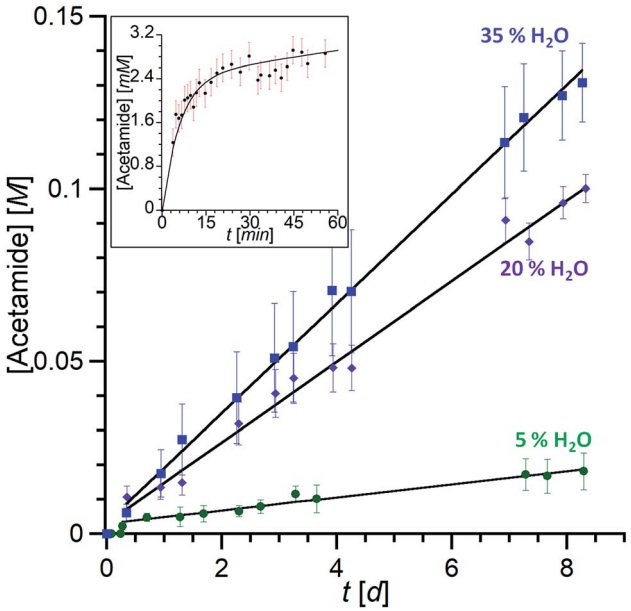

Fig. 8 Kinetic traces of acetamide formation. [Rim_4Zn] = 3 mM, acetonitrile, 70 °C. Total formation of acetamide (free and *endo*-bound) over several days with different water contents (measured by ^{1}H NMR (CH_3CN/CD_3CN = 4 : 1)). Inset: burst phase with the formation of the acetamido *endo* complex followed by integration of the ^{1}H NMR trace at $\delta = -2.4$ ppm (20% H_2O). The data are fitted according to the equation corresponding to the classical model for reaction inhibition due to product displacement (see the ESI†).[36]

Table 2 Reaction rates calculated (with a two-phase kinetic model)[36] at various complex concentrations and water contents. v_1 corresponds to the initial burst phase and v_2 to the stationary phase that follows[a]

[Rim_4Zn] (mM)	% H_2O	T (°C)	v_1 (10^{-3} M min^{-1})	v_2 (10^{-6} M min^{-1})
3	5	70	0.4 ± 0.1	2 ± 1
3	20	70	0.5 ± 0.1	8 ± 2
6	20	70	1.1 ± 0.2	nd
3	35	70	0.5 ± 0.1	11 ± 2

[a] nd = not determined.

spectroscopy, and in comparison to the rate of hydration). Knowing that one imidazole arm of complex B is hemilabile, it is likely that a fast equilibrium also exists between species B and C where the 4th imidazole arm is substituted by a water molecule.‡‡ The corresponding complex C presents in the *cis* position an acetonitrile guest substrate and a water ligand, the latter becoming acidic due its coordination to Zn^{II}. The free imidazole arm can then act as a base for the activation of the water ligand[37,38] and its nucleophilic addition to the polarized nitrile that sits in close proximity. The resulting complex D is the complex observed during the reaction course, in the stationary state. The equilibrium between species D and E is the most probable pathway for the substitution of acetamide (or the corresponding iminol, a neutral and thus labile ligand in E) by the solvent. This allows the regeneration of the initial form of the catalyst.

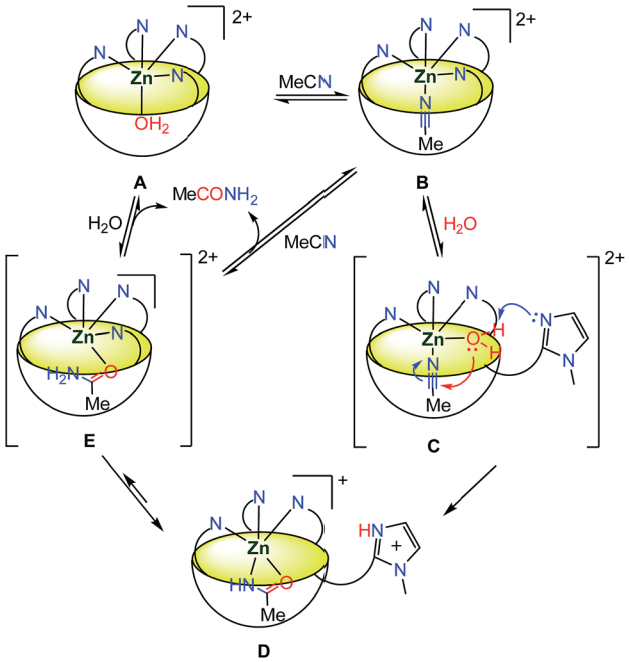

Scheme 3 Proposed mechanism for the hydration of MeCN catalyzed by Rim_4Zn.

The kinetic study highlighted two different phases. At first, during the burst phase, A and B being in fast equilibrium, the limiting step is within B → C → D. The absence of noticeable KIE with D_2O does not allow the identification of the rate determining step. In the second (slow) phase, a turn-over of 0.22 h^{-1} was observed at 70 °C and 35% water content. Under these conditions, it reached a TON of 43 after 198 hours with a 3 mM catalyst concentration. The slowness of the catalysis (the reaction rate v_2 is two orders of magnitude lower than v_1) is proposed to be due to the relatively strong binding of acetamide as an anion [$K = (1.2 \pm 0.5) \times 10^3$ M^{-1} in a 95 : 5 v/v MeCN/D_2O mixture, see ESI Fig. S31†] that must be displaced through a sequence involving protonation and exchange for acetonitrile.

Nitrile hydration is a challenging process since the nitrilo function is a poor electrophile (especially acetonitrile) and water a poor nucleophile. Nature provides nitrile hydratases, which are metallo-enzymes that combine the activation of the nitrilo substrate by coordination to Fe^{III} or Co^{III} to the attack of a coordinated sulfenate (derived from a cysteine residue) on either the water molecule (thus acting as an internal base)[37,38] or directly onto the substrate.[39] Although the biomimetic approach has led to the synthesis of a great variety of metal complexes, a relatively small number has been reported as active catalysts for the hydration of acetonitrile.[40–42] With mononuclear Co^{III} complexes based on tetraaza ligands, simultaneous coordination of the nitrile and water molecules in the *cis*-position has been proposed to explain the efficiency of the catalyst.[43,44] This route was also suggested by theoretical studies on Zn^{II}-exchanged zeolites.[45]

Most efficient catalysts are based on metals not following a biomimetic approach, with the drawback of poor selectivity (*vs.* substrate as there is no substrate recognition step, and *vs.* products), as often hydrolysis follows the hydration step.[46–51]

Relatively recently however, the so-called bifunctional catalysts have been reported for the hydration of nitriles.[52–56] These catalysts either employ a heteroatom in the ligand backbone to direct the water attack to the nitrile carbon atom, or use a hemilabile basic group for water activation. They are based mostly on precious metals such as Ru, Rh or Pt, although a very recent report describes a Ni^{II} catalyst displaying hemilability-driven water activation for the hydration of a coordinated nitrile.[57] Examples of biomimetic Zn^{II} catalysts are very rare.[6–13,43,44] One of the most efficient is a ketoxime complex, which is proposed to act as a nucleophilic catalyst.[58] Finally, it is worth noting that none of these catalysts involves molecular recognition through cavity binding. Breslow reported a CD functionalized by an oximate–nickel complex that is active for the catalytic hydrolysis of activated esters *via* transient nucleophilic attack of the cavity-hosted substrate by the oximate ligand, but not for nitrile hydration.[59]

Conclusions

Here, we have described the synthesis of a new ligand based on a resorcinarene macrocycle rigidified into a bowl structure by methylene bridges between the resorcinol units. It presents a tetra(imidazole) coordination core at the large rim of the bowl structure. Such an environment allows the formation of mononuclear Zn^{II} complexes with a well-defined coordination sphere displaying an *endo* site available for the inclusion of a guest ligand. In acetonitrile, it is occupied by a molecule of solvent that can be readily displaced by anionic guests. The most important new features, when compared to the **Rim$_3$**-based Zn^{II} complex, stem from the presence of the 4th imidazole arm that is hemilabile. This latter can be selectively protonated without disruption of the Zn^{II} environment, keeping its "bowl-complex" structure and *endo*-hosting properties. Such a property finds a direct application through the reaction of the dicationic nitrilo complex with acidic guests. The combination of the coordination of the ligand to the Lewis acidic Zn^{II} center with its deprotonation by the 4th imidazole arm allows direct binding of carboxylic acids, β-diketones and even acetamide, under the control of the *endo*-binding site. An important consequence of such acido-basic/hemilabile features relates to the reactivity of the metal center as illustrated here with the hydration of acetonitrile. Indeed, the **Rim$_4$**Zn^{II} complex has been shown to catalyze the formation of acetamide when dissolved in MeCN in the presence of various amounts of water. Preliminary kinetic studies evidence biphasic kinetics. An initial burst phase corresponds to the fast appearance of *endo*-bound acetamide ($t_{1/2}$ = 4 min at 70 °C), which is followed by a slow phase attributed to slow product release. A general base assistance behavior is proposed to explain the efficiency of the initial burst phase.

In spite of its moderate activity relative to precious metal-based catalysts,[52–57] this complex displays highly significant and unique biomimetic features relative to the water activation process in hydrolytic Zn enzymes. Indeed, this is the first time that the following criteria are put forward:

(i) A biomimetic 1st coordination sphere (three imidazole groups),

(ii) *cis*-coordination availability for two exogenous molecules,

(iii) basic assistance by an imidazole group acting as an internal base, and

(iv) the cavity effect for substrate and product binding.

This leads to spectacular assistance for acidic guest binding (*e.g.* $MeCONH_2$) and acetonitrile hydration (a rare example of a Zn^{II} based catalyst).

We are now further exploring the mechanism through in-depth kinetic studies and theoretical modeling as well as reactivity with other metal ions and other substrates with which cavity binding and general base assistance may be key features.

Conflicts of interest

There are no conflicts to declare.

Acknowledgements

This project was supported by the CNRS (Institut de Chimie) and the Ministère de l'Enseignement Supérieur et de la Recherche. The COST Action CM1005 "Supramolecular Chemistry in Water" is kindly acknowledged for supporting scientific discussions and short-term scientific missions. G. B. acknowledges the Belgian FNRS (FRFC 2010: 2.4592.10F) and the van Buuren Foundation for the funding of the ITC equipment. The authors thank Dr Lionel Marcelis for fruitful discussions about kinetics and NMR analyses.

Notes and references

‡ Likewise, the diffusion coefficients obtained for **Rim$_3$** and **Rim$_3$**Zn are very similar (8.2×10^{-10} and 8.0×10^{-10} m^2 s^{-1}, respectively).

§ The reverse titration with **Rim$_3$**, monitored *via* ITC, gave the same results as the direct one, which was not the case for **Rim$_4$**. Due to the fourth imidazole, an excess of zinc may have an effect on the protonation form of the ligand, which results in a phenomenon different from complexation.

¶ The pK_a value was calculated considering the following equilibrium: [**Rim$_4$**-Zn(S)]$^{2+}$ + PicH ⇔ [**Rim$_4$**Zn(S)H]$^{3+}$ + Pic$^-$, which results from the reaction of two acid/base couples [pK_a(PicH) in MeCN = 11]. The associated constant K in acetonitrile can thus be written as $K = K_{a,PicH/Pic^-}/K_{a,[\mathbf{Rim4}ZnH]^{3+}/[\mathbf{Rim4}Zn]^{2+}}$, from which $K_{a,[\mathbf{Rim4}ZnH]^{3+}/[\mathbf{Rim4}Zn]^{2+}}$ is deduced.

‖ Compared pK_a values in DMSO: imidazolium: 6.4; AcOH: 12.3; acetylacetone: 13.5; $AcNH_2$: 25.5 (values from the Bordwell pK_a table). The corresponding values in MeCN have not been reported.

** With all acidic guests (GH = RCO_2H, $MeCONH_2$, and $MeCOCH_2COMe$), the δ shift of added Et_3N showed its quantitative protonation. A detailed structural analysis of the acetamido complex is currently under investigation, as well as the kinetics of its binding, which is slow under anhydrous conditions, and fast in the presence of water. These studies will be the subject of another article.

†† The mono-cationic complexes obtained with β-diketones and Et_3N present most probably a pending imidazole arm that is in rapid exchange with the three-coordinated one.

‡‡ This was substantiated by an NMR experiment where the gradual addition of water to a solution of [**Rim$_4$**Zn(OAc)](ClO_4) in CD_3CN led to the appearance of new peaks in the low- and high-field regions, thereby attesting to the formation of a solvated (by water) species. See ESI Fig. S22.†

1 G. Parkin, *Chem. Rev.*, 2004, **104**, 699–768.
2 D. Desbouis, I. P. Troitsky, M. J. Belousoff, L. Spiccia and B. Graham, *Coord. Chem. Rev.*, 2012, **256**, 897–937.

3 M. Zhao, H.-B. Wang, L.-N. Ji and Z.-W. Mao, *Chem. Soc. Rev.*, 2013, **42**, 8360.
4 K. E. Dalle and F. Meyer, *Eur. J. Inorg. Chem.*, 2015, 3391–3405.
5 T. Joshi, B. Graham and L. Spiccia, *Acc. Chem. Res.*, 2015, **48**, 2366–2379.
6 H. Aït-Haddou, J. Sumaoka, S. L. Wiskur, J. F. Folmer-Andersen and E. V. Anslyn, *Angew. Chem.*, 2002, **114**, 4185–4188.
7 G. Feng, J. C. Mareque-Rivas, R. Torres Martín de Rosales and N. H. Williams, *J. Am. Chem. Soc.*, 2005, **127**, 13470–13471.
8 R. A. Allred, K. Doyle, A. M. Arif and L. M. Berreau, *Inorg. Chem.*, 2006, **45**, 4097–4108.
9 M. Livieri, F. Mancin, U. Tonellato and J. Chin, *Chem. Commun.*, 2004, 2862.
10 E. Y. Tirel, Z. Bellamy, H. Adams, V. Lebrun, F. Duarte and N. H. Williams, *Angew. Chem., Int. Ed.*, 2014, **53**, 8246–8250.
11 E. Y. Tirel and N. H. Williams, *Chem.–Eur. J.*, 2015, **21**, 7053–7056.
12 G. Feng, J. C. Mareque-Rivas and N. H. Williams, *Chem. Commun.*, 2006, 1845.
13 M. Livieri, F. Mancin, G. Saielli, J. Chin and U. Tonellato, *Chem.–Eur. J.*, 2007, **13**, 2246–2256.
14 D. Coquière, S. Le Gac, U. Darbost, O. Sénèque, I. Jabin and O. Reinaud, *Org. Biomol. Chem.*, 2009, **7**, 2485.
15 N. Le Poul, Y. Le Mest, I. Jabin and O. Reinaud, *Acc. Chem. Res.*, 2015, **48**, 2097–2106.
16 J.-N. Rebilly, B. Colasson, O. Bistri, D. Over and O. Reinaud, *Chem. Soc. Rev.*, 2015, **44**, 467–489.
17 J.-N. Rebilly and O. Reinaud, *Supramol. Chem.*, 2014, **26**, 454–479.
18 A. Višnjevac, J. Gout, N. Ingert, O. Bistri and O. Reinaud, *Org. Lett.*, 2010, **12**, 2044–2047.
19 N. Natarajan, E. Brenner, D. Sémeril, D. Matt and J. Harrowfield, *Eur. J. Org. Chem.*, 2017, 6100–6113.
20 D. S. Auld, *BioMetals*, 2001, **14**, 271–313.
21 A. Messerschmidt, W. Bode and M. Cygler, *Handbook of Metalloproteins*, Wiley, 2004, vol. 3.
22 D. W. Christianson and W. N. Lipscomb, *Acc. Chem. Res.*, 1989, **22**, 62–69.
23 W. N. Lipscomb and N. Sträter, *Chem. Rev.*, 1996, **96**, 2375–2434.
24 N. Cerdà-Costa and F. Xavier Gomis-Rüth, *Protein Sci.*, 2014, **23**, 123–144.
25 M. Hernick and C. A. Fierke, *Arch. Biochem. Biophys.*, 2005, **433**, 71–84.
26 M. S. Finnin, J. R. Donigian, A. Cohen, V. M. Richon, R. A. Rifkind, P. A. Marks, R. Breslow and N. P. Pavletich, *Nature*, 1999, **401**, 184–188.
27 F. Fonseca, E. H. C. Bromley, M. J. Saavedra, A. Correia and J. Spencer, *J. Mol. Biol.*, 2011, **411**, 951–959.
28 D. K. Wilson, F. B. Rudolph and F. A. Quiocho, *Science*, 1991, **252**, 1278–1284.
29 H. E. Moll, D. Sémeril, D. Matt, M.-T. Youinou and L. Toupet, *Org. Biomol. Chem.*, 2009, **7**, 495–501.
30 J. Gout, A. Višnjevac, S. Rat, O. Bistri, N. Le Poul, Y. Le Mest and O. Reinaud, *Eur. J. Inorg. Chem.*, 2013, 5171–5180.
31 A. Kütt, I. Leito, I. Kaljurand, L. Sooväli, V. M. Vlasov, L. M. Yagupolskii and I. A. Koppel, *J. Org. Chem.*, 2006, **71**, 2829–2838.
32 I. Kaljurand, A. Kütt, L. Sooväli, T. Rodima, V. Mäemets, I. Leito and I. A. Koppel, *J. Org. Chem.*, 2005, **70**, 1019–1028.
33 J. Gout, S. Rat, O. Bistri and O. Reinaud, *Eur. J. Inorg. Chem.*, 2014, 2819–2828.
34 *HyperChem Professional Release 7*, HyperCube Inc., 1115 NW 4th St, Gainesville, FL 32601, USA.
35 Y.-H. Cho and H.-S. Shin, *Anal. Chim. Acta*, 2013, **787**, 111–117.
36 C. Frieden, *J. Biol. Chem.*, 1970, **245**, 5788–5799.
37 K. Hashimoto, H. Suzuki, K. Taniguchi, T. Noguchi, M. Yohda and M. Odaka, *J. Biol. Chem.*, 2008, **283**, 36617–36623.
38 S. Mitra and R. C. Holz, *J. Biol. Chem.*, 2007, **282**, 7397–7404.
39 M. T. Nelp, Y. Song, V. H. Wysocki and V. Bandarian, *J. Biol. Chem.*, 2016, **291**, 7822–7829.
40 F. Meyer, E. Kaifer, P. Kircher, K. Heinze and H. Pritkow, *Chem.–Eur. J.*, 1999, **5**, 1617–1630.
41 P. J. Zinn, T. N. Sorrell, D. R. Powell, V. W. Day and A. S. Borovik, *Inorg. Chem.*, 2007, **46**, 10120–10132.
42 L. M. Berreau and W. B. Tolman, *Activation of Small Molecules: Organometallic and Bioinorganic Perspectives*, Wiley VCH, 2006.
43 J. H. Kim, J. Britten and J. Chin, *J. Am. Chem. Soc.*, 1993, **115**, 3618–3622.
44 J. Chin, *Acc. Chem. Res.*, 1991, **24**, 145–152.
45 L. A. Barbosa and R. A. van Santen, *J. Mol. Catal. Chem.*, 2001, **166**, 101–121.
46 V. Y. Kukushkin and A. J. L. Pombeiro, *Chem. Rev.*, 2002, **102**, 1771–1802.
47 V. Y. Kukushkin and A. J. L. Pombeiro, *Inorg. Chim. Acta.*, 2005, **358**, 1–21.
48 T. J. Ahmed, S. M. M. Knapp and D. R. Tyler, *Coord. Chem. Rev.*, 2011, **255**, 949–974.
49 R. García-Álvarez, P. Crochet and V. Cadierno, *Green Chem.*, 2013, **15**, 46–66.
50 R. García-Álvarez, J. Francos, E. Tomás-Mendivil, P. Crochet and V. Cadierno, *J. Organomet. Chem.*, 2014, **771**, 93–104.
51 R. González-Fernández, P. Crochet, V. Cadierno, M. I. Menéndez and R. López, *Chem.–Eur. J.*, 2017, **23**, 15210–15221.
52 P. Daw, A. Sinha, S. M. W. Rahaman, S. Dinda and J. K. Bera, *Organometallics*, 2012, **31**, 3790–3797.
53 T. Šmejkal and B. Breit, *Organometallics*, 2007, **26**, 2461–2464.
54 M. Muranaka, I. Hyodo, W. Okumura and T. Oshiki, *Catal. Today*, 2011, **164**, 552–555.
55 D. B. Grotjahn, *Chem.–Eur. J.*, 2005, **11**, 7146–7153.
56 T. Oshiki, H. Yamashita, K. Sawada, M. Utsunomiya, K. Takahashi and K. Takai, *Organometallics*, 2005, **24**, 6287–6290.
57 K. Singh, A. Sarbajna, I. Dutta, P. Pandey and J. K. Bera, *Chem.–Eur. J.*, 2017, **23**, 7761–7771.
58 M. N. Kopylovich, V. Y. Kukushkin, M. Haukka, J. J. R. Fraústo da Silva and A. J. L. Pombeiro, *Inorg. Chem.*, 2002, **41**, 4798–4804.
59 R. Breslow and S. D. Dong, *Chem. Rev.*, 1998, **98**, 1997–2012.